

Neutrinos from WIMP annihilation in the Sun : Implications of a self-consistent model of the Milky Way’s dark matter halo

Susmita Kundu* and Pijushpani Bhattacharjee†

*AstroParticle Physics & Cosmology Division and Centre for AstroParticle Physics,
Saha Institute of Nuclear Physics, 1/AF Bidhannagar, Kolkata 700064, India*

Upper limits on the spin-independent (SI) as well as spin-dependent (SD) elastic scattering cross sections of low mass ($\sim 2 - 20$ GeV) WIMPs (Weakly Interacting Massive Particles) with protons, imposed by the upper limit on the neutrino flux from WIMP annihilation in the Sun given by the Super-Kamiokande (S-K) experiment, and their compatibility with the “DAMA-compatible” regions of the WIMP parameter space — the regions of the WIMP mass versus cross section parameter space within which the annual modulation signal observed by the DAMA/LIBRA experiment is compatible with the null results of other direct detection experiments — are studied within the frame work of a self-consistent model of the finite-size dark matter (DM) halo of the Galaxy. The halo model includes the gravitational influence of the observed visible matter of the Galaxy on the phase space distribution function of the WIMPs constituting the Galaxy’s DM halo in a self-consistent manner. Unlike in the “Standard Halo Model” (SHM) used in earlier analyses, the velocity distribution of the WIMPs in our model is non-Maxwellian, with a high-velocity cutoff determined self-consistently by the model itself. The parameters of the model are determined from a fit to the rotation curve data of the Galaxy. We find that, for our best fit halo model, for SI interaction, while the S-K upper limits do not place additional restrictions on the DAMA-compatible region of the WIMP parameter space if the WIMPs annihilate dominantly to $\bar{b}b$ and/or $\bar{c}c$, portions of the DAMA-compatible region can be excluded if WIMP annihilations to $\tau^+\tau^-$ and $\nu\bar{\nu}$ occur at larger than 35% and 0.4% levels, respectively. For SD interaction, on the other hand, the restrictions on the possible annihilation channels are much more stringent: they rule out the entire DAMA region if WIMPs annihilate to $\tau^+\tau^-$ and $\nu\bar{\nu}$ final states at greater than $\sim 0.05\%$ and 0.0005% levels, respectively, and/or to $\bar{b}b$ and $\bar{c}c$ at greater than $\sim 0.5\%$ levels. The very latest results from the S-K Collaboration [T. Tanaka et al, *Astrophys. J.* **742**:78 (2011)] make the above constraints on the branching fractions of various WIMP annihilation channels even more stringent by roughly a factor of 3–4.

* susmita.kundu@saha.ac.in

† pijush.bhattacharjee@saha.ac.in

I. INTRODUCTION

Weakly Interacting Massive Particles (WIMPs) (hereafter generically denoted by χ) with masses m_χ in the range of few GeV to few TeV are a natural candidate for the dark matter (DM) in the Universe; See e.g., Refs. [1–5] for reviews. Several experiments are currently engaged in efforts to directly detect such WIMPs by observing nuclear recoils due to scattering of WIMPs off nuclei in suitably chosen detector materials in underground laboratories. Recent results from some of these direct detection (DD) experiments, in particular the annual modulation of the nuclear recoil event rates reported by the DAMA/LIBRA collaboration [6] and the excess of low energy recoil events reported by the CoGeNT collaboration [7] have raised the interesting possibility [8, 9] that these events could be due to WIMPs of relatively low mass, approximately in the range $\sim 5\text{--}10$ GeV, interacting with nuclei with a WIMP-nucleon spin-independent elastic cross section in the region of few $\times 10^{-4}$ pb, without conflicting with the null results from other experiments such as XENON10 [10], XENON100 [11] and CDMS-II-Si [12]. Earlier analyses (before the CoGeNT results [7]) had also found similar compatibility of the DAMA/LIBRA annual modulation signal with the null results from other DD experiments; see, e.g., Refs. [13–15].¹

Scattering of WIMPs off nuclei can also lead to capture of the WIMPs by massive astrophysical bodies such as the Sun or the Earth if, after scattering off a nucleus inside the body, the velocity of the WIMP falls below the escape velocity of the body. The WIMPs so captured over the lifetime of the capturing body would gradually settle down to the core of the body where they would annihilate and produce standard model particles, e.g., W^+W^- , Z^0Z^0 , $\tau^+\tau^-$, $t\bar{t}$, $b\bar{b}$, $c\bar{c}$, etc. Decays of these particles would then produce neutrinos, gamma rays, electrons-positrons, protons-antiprotons, etc. For astrophysical objects like the Sun or the Earth, only the neutrinos would be able to escape. Detection of these neutrinos by large neutrino detectors can, albeit indirectly, provide a signature of WIMPs. Although no detection has yet been reported, the Super-Kamiokande (S-K) detector, for example, has provided upper limits on the possible neutrino flux from WIMP annihilation in the Sun as a function of the WIMP mass [18–20]. Similarly, the γ -rays produced in the annihilation of the WIMPs in suitable astrophysical environments with enhanced DM density but low optical depth to gamma rays, such as in the central region of our Galaxy, in dark matter dominated objects such as dwarf galaxies, and in clusters of galaxies, can offer a complimentary avenue of indirect detection (ID) of WIMPs. Although no unambiguous gamma ray signals of dark matter origin have been reported, a recent analysis [21] of the spectral and morphological features of the gamma ray emission from the inner Galactic Center region (within a Galactocentric radius of ~ 175 pc) measured by the Fermi Gamma-ray Space Telescope (FGST) seems to suggest the presence of a gamma ray emission component which is difficult to explain in terms of known sources and/or process of gamma ray production, but is consistent with that expected from annihilations of WIMPs of mass in the 7–9 GeV range (annihilating primarily to tau leptons) with a suitably chosen density and distribution of the dark matter in the Galactic Center region; see, however, Ref. [22] for a different view.

In this paper we focus on the neutrinos produced by annihilations of WIMPs in the core of the Sun, and study the constraints imposed on the WIMP mass vs. WIMP-nucleon cross section, for low-mass ($\lesssim 20$ GeV) WIMPs, from non-detection of such neutrinos. This is done within the context of a self-consistent model of the finite-size dark halo of the Galaxy [15, 23] that includes the gravitational effect of the observed visible matter on the DM in a self-consistent manner, with the parameters of the model determined from fits to the rotation curve data of the Galaxy [24, 25].

The expected flux of neutrinos from the Sun due to WIMP annihilations depends on the rate at which WIMPs are captured by the Sun. The capture rate depends on the density as well as the velocity distribution of the WIMPs in the solar neighborhood as the Sun goes around the Galaxy. The density and velocity distribution of the WIMPs in the Galaxy are *a priori* unknown. Most earlier studies of neutrinos from WIMP capture and annihilation in the Sun have been done within the context of the so-called “Standard Halo Model” (SHM) in which the DM halo of the Galaxy is described by a single component isothermal sphere [26] with a Maxwellian velocity distribution of the DM particles in the Galactic rest frame [1, 27, 28]). The velocity distribution is isotropic, and is usually truncated at a chosen value of the escape speed of the Galaxy. The density of DM in the solar neighborhood is typically taken to be in the range $\rho_{\text{DM},\odot} \sim 0.3 \pm 0.1 \text{ GeV}/\text{cm}^3$ [29–32]². The velocity dispersion, $\langle v^2 \rangle^{1/2}$, the parameter characterizing the Maxwellian velocity distribution of the SHM, is typically taken to be $\sim 270 \text{ km s}^{-1}$. This follows from the relation [26],

¹ The question of compatibility of the DAMA/LIBRA and CoGeNT results with the null results of other experiments, however, remains controversial; see, e.g., the results of a recent reanalysis of the CDMS-II Germanium data with a lowered recoil-energy threshold of 2 keV [16], as well as the recent results from the XENON100 collaboration [17], both of which claim to disfavor such a compatibility.

² See, however, recent analyses [33, 34] which claim a value closer to $0.4 \text{ GeV}/\text{cm}^3$ with uncertainty $\lesssim 10\%$.

$\langle v^2 \rangle^{1/2} = \sqrt{\frac{3}{2}} v_{c,\infty}$, between the velocity dispersion of the particles constituting a single-component self-gravitating isothermal sphere and the asymptotic value of the circular rotation speed, $v_{c,\infty}$, of a test particle in the gravitational field of the isothermal sphere and assuming $v_{c,\infty} \approx v_{c,\odot} \approx 220 \text{ km s}^{-1}$, where $v_{c,\odot}$ is the measured value of the circular rotation velocity of the Galaxy in the solar neighborhood.³ Neutrino flux from DM annihilation in the Sun for low mass WIMPs and the resulting constraints on WIMP properties from the Super-Kamiokande upper limits on such neutrinos have been studied within the context of the SHM in Refs. [19, 36–38], which showed that the Super-Kamiokande upper limits on the possible flux of neutrinos from the Sun place stringent restrictions on the DAMA region of the WIMP parameter space.

Whereas the SHM serves as a useful benchmark model, there are a number of reasons why the SHM does not provide a satisfactory description of the dynamics of the Galaxy. First, it does not take into account the modification of the phase space structure of the DM halo due to the significant gravitational effect of the observed visible matter on the DM particles inside and up to the solar circle. Second, the isothermal sphere model of the halo is infinite in extent and has a formally divergent mass, with mass inside a radius r , $M(r) \propto r$, as $r \rightarrow \infty$, and is thus unsuitable for representing a halo of finite size. Third, the procedure of truncating the Maxwellian speed distribution at a chosen value of the local (solar neighborhood) escape speed is not a self-consistent one because the resulting speed distribution is not in general a self-consistent solution of the steady-state collisionless Boltzmann equation describing a finite system of collisionless DM particles. In addition, since the rotation curve for such a truncated Maxwellian is, in general, not asymptotically flat, the relation $\langle v^2 \rangle^{1/2} = \sqrt{\frac{3}{2}} v_{c,\infty}$ used to determine the value of $\langle v^2 \rangle^{1/2}$ in the Maxwellian speed distribution of the isothermal sphere, as done in the SHM, is not valid in general. Finally, recent numerical simulations [32] seem to find that the velocity distribution of the Dark Matter particles deviates significantly from the usual Maxwellian form. These issues are further discussed in detail in Ref. [15], where we discussed a self-consistent model of the finite-size dark halo of the Galaxy that avoids the above mentioned inconsistencies of the SHM and also studied the constraints on WIMP properties from the results of the direct detection (DD) experiments within the context of this self-consistent halo model. It is of interest to extend this study to the case of indirect detection (ID) of WIMPs via neutrinos from WIMP annihilations in the Sun, which is the purpose of this paper.

Our model of the phase space structure of the finite-size DM halo of the Galaxy is based on the so-called “lowered” (or truncated) isothermal models (often called “King models”) [26] of the phase-space distribution function (DF) of collisionless particles. These models are proper self-consistent solutions of the collisionless Boltzmann equation representing nearly isothermal systems of finite physical size and mass. There are two important features of these models: First, at every location within the system a DM particle can have speeds up to a maximum speed which is self-consistently determined by the model itself. A particle of maximum velocity at any location within the system can just reach its outer boundary, fixed by the truncation radius, a parameter of the model, where the DM density by construction vanishes. Second, the speed distribution of the particles constituting the system is non-Maxwellian. To include the gravitational effect of the observed visible matter on the DM particles, we modify the “pure” King model DF by replacing the gravitational potential appearing in the King model DF by the total gravitational potential consisting of the sum of those due to DM and the observed visible matter. This interaction with the visible matter influences both the density profile and the velocity distribution of the dark matter particles as compared to those for a “pure” King model. In particular, the dark matter is pulled in by the visible matter, thereby increasing its central density significantly. When the visible matter density is set to zero and the truncation radius is set to infinity, our halo model becomes identical to that of a single-component isothermal sphere used in the SHM. For further discussion of the model, see [15, 23].

The DM distribution in the Galaxy may have significant amount of substructures which may have interesting effects on the WIMP capture and annihilation rates [39]. However, not much information, based on observational data, is available about the spatial distribution and internal structures of these substructures. As such, in this paper we shall be concerned only with the smooth component of the DM distribution in the Galaxy described by our self-consistent model mentioned above, the parameters of which are determined from the observed rotation curve data for the Galaxy.

The non-Maxwellian nature of the WIMP speed distribution in our halo model makes the calculation of the WIMP

³ A somewhat higher value of $v_{c,\odot} \approx 250 \text{ km s}^{-1}$, as suggested by a recent study [35], would imply a correspondingly higher value of $\langle v^2 \rangle^{1/2}_{\text{iso}} \approx 306 \text{ km s}^{-1}$.

capture (and consequently annihilation) rate non-trivial since the standard analytical formula for the capture rate given by Gould [40] and Press and Spergel [41], which is widely used in the literature, is not valid for the non-Maxwellian speed distribution in our halo model, and as such has to be calculated ab initio; see section III.

We calculate the 90% C.L. upper limits on the WIMP-proton spin-independent (SI) as well as spin-dependent (SD) elastic cross sections as a function of the WIMP mass, for various WIMP annihilation channels, using the 90% C.L. upper limits on the rates of upward-going muon events due to neutrinos from Sun derived from the results of S-K collaboration ([18], [19] and references therein).⁴ We then study the consistency of those limits with the 90% C.L. “DAMA-compatible” regions — the regions of the WIMP mass versus cross section parameter space within which the annual modulation signal observed by the DAMA/LIBRA experiment [6] is compatible with the null results of other DD experiments — determined within the context of our halo model [15]. We find that the requirement of such consistency imposes stringent restrictions on the branching fractions of the various WIMP annihilation channels. For example, in the case of spin-independent WIMP-proton interaction, while the S-K upper limits do not place additional restrictions on the DAMA-compatible region of the WIMP parameter space if the WIMPs annihilate dominantly to $\bar{b}b$, $\bar{c}c$, portions of the DAMA-compatible region can be excluded if WIMP annihilations to $\tau^+\tau^-$ and $\nu\bar{\nu}$ occur at larger than 35% and 0.4% levels, respectively. In the case of spin-dependent interactions, on the other hand, the restrictions on the branching fractions of various annihilation channels are much more stringent. Specifically, they rule out the entire DAMA region if WIMPs annihilate to $\tau^+\tau^-$ and $\nu\bar{\nu}$ final states at greater than $\sim 0.05\%$ and 0.0005% levels, respectively, and/or to $\bar{b}b$ and $\bar{c}c$ at greater than $\sim 0.5\%$ levels.⁵ The very latest results from the S-K Collaboration [20] make the above constraints on the branching fractions of various WIMP annihilation channels even more stringent by roughly a factor of 3–4.

The rest of the paper is organized as follows: In section II we briefly describe the self-consistent model of the DM halo of the Galaxy. The formalism of calculating the WIMP capture and annihilation rates in the Sun within the context of our DM halo model, and that for calculating the resulting neutrino flux and event rate in the Super-Kamiokande detector, are discussed in sections III and IV, respectively. Our results and the constraints on the WIMP properties implied by these results are described in section V. The paper ends with a Summary in section VI.

II. THE SELF-CONSISTENT TRUNCATED ISOTHERMAL MODEL OF THE MILKY WAY’S DARK MATTER HALO

The phase space distribution function (DF) of the DM particles constituting a truncated isothermal halo of the Galaxy can be taken, in the rest frame of the Galaxy, to be of the “King model” form [15, 23, 26],

$$f(\mathbf{x}, \mathbf{v}) \equiv f(\mathcal{E}) = \begin{cases} \rho_1 (2\pi\sigma^2)^{-3/2} \left(e^{\mathcal{E}/\sigma^2} - 1 \right) & \text{for } \mathcal{E} > 0, \\ 0 & \text{for } \mathcal{E} \leq 0, \end{cases} \quad (1)$$

where

$$\mathcal{E}(\mathbf{x}) \equiv \Phi(r_t) - \left(\frac{1}{2}v^2 + \Phi(\mathbf{x}) \right) \equiv \Psi(\mathbf{x}) - \frac{1}{2}v^2, \quad (2)$$

is the so-called “relative energy” and $\Psi(\mathbf{x}) = -\Phi(\mathbf{x}) + \Phi(r_t)$ the “relative potential”, $\Phi(\mathbf{x})$ being the total gravitational potential under which the particles move, with boundary condition $\Phi(0) = 0$. The relative potential and relative energy, by construction, vanish at $|\mathbf{x}| = r_t$, the truncation radius, which represents the outer edge of the system where the particle density vanishes. At any location \mathbf{x} the maximum speed a particle of the system can have is

$$v_{\max}(\mathbf{x}) = \sqrt{2\Psi(\mathbf{x})}, \quad (3)$$

⁴ After the completion of the main calculations of the present work, new results of the S-K collaboration’s search for upward-going muons due to neutrinos from Sun [20] have appeared. We include, at the end of section V, a discussion of the new results of Ref. [20] and the resulting constraints on various WIMP annihilation channels.

⁵ In the present paper, the CoGeNT results [7] are not included in the analysis. Preliminary results of the analysis [42] to find the “CoGeNT-compatible” region in the WIMP mass vs. cross section plane *within the context of our halo model* indicates that its inclusion will not significantly change the above constraints on the branching fractions for the various annihilation channels.

at which the relative energy \mathcal{E} and, as a consequence, the DF (1), vanish. The model has three parameters, namely, ρ_1 , σ and r_t . Note that the parameter σ in the King model is not same as the usual velocity dispersion parameter of the isothermal phase space DF [26]. Also, in our calculations below, we shall use the parameter $\rho_{\text{DM},\odot}$, the value of the DM density at the location of the Sun, in place of the parameter ρ_1 .

Integration of $f(\mathbf{x}, \mathbf{v})$ over all velocities gives the DM density at the position \mathbf{x} :

$$\rho_{\text{DM}}(\mathbf{x}) = \frac{\rho_1}{(2\pi\sigma^2)^{3/2}} \int_0^{\sqrt{2\Psi(\mathbf{x})}} dv 4\pi v^2 \left[\exp\left(\frac{\Psi(\mathbf{x}) - v^2/2}{\sigma^2}\right) - 1 \right] \quad (4)$$

$$= \rho_1 \left[\exp\left(\frac{\Psi(\mathbf{x})}{\sigma^2}\right) \text{erf}\left(\frac{\sqrt{\Psi(\mathbf{x})}}{\sigma}\right) - \sqrt{\frac{4\Psi(\mathbf{x})}{\pi\sigma^2}} \left(1 + \frac{2\Psi(\mathbf{x})}{3\sigma^2}\right) \right], \quad (5)$$

which satisfies the Poisson equation

$$\nabla^2 \Phi_{\text{DM}}(\mathbf{x}) = 4\pi G \rho_{\text{DM}}(\mathbf{x}), \quad (6)$$

where Φ_{DM} is the contribution of the DM component to the total gravitational potential,

$$\Phi(\mathbf{x}) = \Phi_{\text{DM}}(\mathbf{x}) + \Phi_{\text{VM}}(\mathbf{x}), \quad (7)$$

in presence of the visible matter (VM) whose gravitational potential, Φ_{VM} , satisfies its own Poisson equation, namely,

$$\nabla^2 \Phi_{\text{VM}}(\mathbf{x}) = 4\pi G \rho_{\text{VM}}(\mathbf{x}). \quad (8)$$

We choose the boundary conditions

$$\Phi_{\text{DM}}(0) = \Phi_{\text{VM}}(0) = 0, \quad \text{and} \quad (\nabla \Phi_{\text{DM}})_{|\mathbf{x}|=0} = (\nabla \Phi_{\text{VM}})_{|\mathbf{x}|=0} = 0. \quad (9)$$

The mass of the system, defined as the total mass contained within r_t , is given by $GM(r_t)/r_t = [\Phi(\infty) - \Phi(r_t)]$. Note that, because of the chosen boundary condition $\Phi(0) = 0$, $\Phi(\infty)$ is a non-zero positive constant.

Since the visible matter distribution $\rho_{\text{VM}}(\mathbf{x})$, and hence the potential $\Phi_{\text{VM}}(\mathbf{x})$, are known from observations and modeling, the solutions of equation (6) together with equations (5), (7) and the boundary conditions (9), give us a three-parameter family of self-consistent pairs of $\rho_{\text{DM}}(\mathbf{x})$ and $\Phi_{\text{DM}}(\mathbf{x})$ for chosen values of the parameters (ρ_1, σ, r_t) . The values of these parameters for the Galaxy can be determined by comparing the theoretically calculated rotation curve, $v_c(R)$, given by

$$v_c^2(R) = R \frac{\partial}{\partial R} [\Phi(R, z=0)] = R \frac{\partial}{\partial R} [\Phi_{\text{DM}}(R, z=0) + \Phi_{\text{VM}}(R, z=0)], \quad (10)$$

with the observed rotation curve data of the Galaxy. (Here R is Galactocentric distance on the equatorial plane and z is the distance normal to the equatorial plane.) This procedure was described in detail in Refs. [15, 23] where, for the visible matter density distribution described there, we determined the values of the parameters r_t and σ that gave reasonably good fit to the rotation curve data of the Galaxy [24, 25] for each of the three chosen values of the parameter $\rho_{\text{DM},\odot} = 0.2, 0.3$ and 0.4 GeV/cm^3 . These models are summarized in Table I, which we use for our calculations in this paper. The density profiles, mass profiles, velocity distributions of the DM particles and the

Model	$\rho_{\text{DM},\odot}$ (GeV/cm ³)	r_t (kpc)	σ (km s ⁻¹)
M1	0.2	120.0	300.0
M2	0.3	80.0	400.0
M3	0.4	80.0	300.0

TABLE I: Parameters of our self-consistent model of the Milky Way's Dark Matter halo that give good fits to the Galaxy's rotation curve data, for the three chosen values of the DM density at the solar neighborhood

resulting rotation curves in each of these models are discussed in detail in Ref. [15].

With our halo model specified, we now briefly review the basic formalism of calculating the WIMP capture and annihilation rates within the context of our halo model.

III. CAPTURE AND ANNIHILATION RATES

The capture rate per unit volume at radius r inside the Sun can be written as [40, 41]

$$\frac{dC}{dV}(r) = \int d^3\mathbf{u} \frac{\tilde{f}(\mathbf{u})}{u} w \Omega^-(w), \quad (11)$$

where $\tilde{f}(\mathbf{u})$ is the WIMP velocity distribution, as measured in the Sun's rest frame, in the neighborhood of the Sun's location in the Galaxy, and $w(r) = \sqrt{u^2 + w_{\text{esc}}(r)}$ is the WIMP's speed at the radius r inside the Sun, $w_{\text{esc}}(r)$ being the escape speed at that radius inside the Sun, which is related to the escape speed at the Sun's core, $w_{\text{esc,core}} \approx 1354 \text{ km s}^{-1}$, and that at its surface, $w_{\text{esc,surf}} \approx 795 \text{ km s}^{-1}$, by the approximate relation

$$w_{\text{esc}}^2(r) = (w_{\text{esc,core}})^2 - \frac{M(r)}{M_{\odot}} [(w_{\text{esc,core}})^2 - (w_{\text{esc,surf}})^2]. \quad (12)$$

The quantity $\Omega^-(w)$ is the capture probability per unit time, which is just the product of the scattering rate and the conditional probability that after a scattering the WIMP's speed falls below the escape speed.

We shall here consider only the elastic scattering of the WIMPs off nuclei. The dominant contribution to the WIMP capture rate will come from the WIMPs scattering off hydrogen and helium nuclei. While for hydrogen, both spin-independent (SI) as well as spin-dependent (SD) cross sections, $\sigma_{\chi p}^{\text{SI}}$ and $\sigma_{\chi p}^{\text{SD}}$, respectively, will contribute, only SI cross section for helium is relevant. (We neglect here the small contribution from ^3He). In general, the effective momentum-transfer (q) dependent WIMP-nucleus SI scattering cross section, $\sigma_{\chi A}^{\text{SI}}(q)$, can be written in the usual way in terms of the “zero-momentum” WIMP-proton (or WIMP-neutron) effective cross section, $\sigma_{\chi p}^{\text{SI}} = \sigma_{\chi n}^{\text{SI}}$, as

$$\sigma_{\chi A}^{\text{SI}}(q) = \frac{\mu_{\chi A}^2}{\mu_{\chi p}^2} \sigma_{\chi p}^{\text{SI}} A^2 |F(q^2)|^2, \quad (13)$$

where A is the number of neutrons plus protons in the nucleus, $\mu_{\chi A}$ and $\mu_{\chi p}$ are the reduced masses of WIMP-nucleus and WIMP-proton systems, respectively, with $\mu_{\chi i} = (m_i m_{\chi})/(m_i + m_{\chi})$, and $F(q^2)$ is the nuclear form-factor (with $F(0) = 1$) which can be chosen to be of the form [1]

$$|F(q^2)|^2 = \exp\left(-\frac{q^2 R^2}{3\hbar^2}\right) = \exp\left(-\frac{\Delta E}{E_0}\right). \quad (14)$$

Here $R \sim \left[0.91 \left(\frac{m_A}{\text{GeV}}\right)^{1/3} + 0.3\right] \times 10^{-13} \text{ cm}$ is the nuclear radius and $E_0 \equiv 3\hbar^2/(2m_A R^2)$ is the characteristic nuclear coherence energy, m_A being the mass of the nucleus.

With the above form of the nuclear form factor, the kinematics of the capture process [40] allows us to write the capture probability per unit time, $\Omega^-(w)$, as

$$\Omega^-(w) = \frac{n_A \sigma_{\chi A}}{w} \frac{2E_0}{m_{\chi}} \frac{\mu_+^2}{\mu} \left[\exp\left(-\frac{m_{\chi} u^2}{2E_0}\right) - \exp\left(-\frac{m_{\chi} w^2}{2E_0} \frac{\mu}{\mu_+}\right) \right] \theta\left(\frac{\mu}{\mu_+^2} - \frac{u^2}{w^2}\right), \quad (15)$$

where n_A is the number density of the scattering nuclei at the radius r inside the Sun, and $\mu \equiv \frac{m_{\chi}}{m_A}$, $\mu_{\pm} \equiv \frac{\mu \pm 1}{2}$. The θ function ensures that those particles which do not lose sufficient amount of energy to be captured are excluded.

We shall use Equation (15) to calculate $\Omega^-(w)$ for helium ($A = 4$). For hydrogen, however, there is no form-factor suppression, and the expression for $\Omega^-(w)$ is simpler:

$$\text{Hydrogen : } \quad \Omega^-(w) = \frac{\sigma_{\chi p} n_H}{w} \left(w_{\text{esc}}^2 - \frac{\mu^2}{\mu} u^2 \right) \theta\left(w_{\text{esc}}^2 - \frac{\mu^2}{\mu} u^2 \right), \quad (16)$$

where n_H is the density of hydrogen (proton) at the radius r inside the Sun. Note that in equations (15) and (16), the quantities w , w_{esc} , n_A and n_H are functions of r .

The WIMP velocity distribution appearing in equation (11) is related to the phase space DF defined in equation (1) (valid in the rest frame of Galaxy) by the Galilean transformation

$$\tilde{f}(\mathbf{u}) = \frac{1}{m_\chi} f(\mathbf{x} = \mathbf{x}_\odot, \mathbf{v} = \mathbf{u} + \mathbf{v}_\odot), \quad (17)$$

where \mathbf{x}_\odot represents the sun's position in the Galaxy ($R = 8.5 \text{ kpc}, z = 0$) and \mathbf{v}_\odot is the Sun's velocity vector *in the Galaxy's rest frame*. Note that Gould's original calculations and the final formula for the WIMP capture rate given in Ref. [40], which are widely used in the literature, use a Maxwellian velocity distribution of the WIMPs in the Galaxy, and as such, cannot directly be used here since the WIMP velocity distribution in our case is non-Maxwellian. In particular, note that the DF f of equation (1) vanishes for speeds $v \geq v_{\text{max}}$ defined in equation (3). Consequently, equation (11) above can be written as

$$\frac{dC}{dV}(r) = \frac{2\pi}{m_\chi} \int_{-1}^1 d(\cos \theta) \int_{u_{\text{min}}=v_\odot}^{u_{\text{max}}(\cos \theta)} u du f(\mathbf{x} = \mathbf{x}_\odot, \mathbf{v} = \mathbf{u} + \mathbf{v}_\odot) w \Omega^-(w), \quad (18)$$

where $v_\odot \approx 220 - 250 \text{ km s}^{-1}$ is the Sun's circular speed in the Galaxy, and u_{max} is given by the positive root of the quadratic equation

$$u_{\text{max}}^2 + v_\odot^2 + 2u_{\text{max}} v_\odot \cos \theta = 2\Psi(\mathbf{x} = \mathbf{x}_\odot). \quad (19)$$

The total WIMP capture rate by the Sun, C_\odot , is given by

$$C_\odot = \int_0^{R_\odot} 4\pi r^2 dr \frac{dC(r)}{dV}, \quad (20)$$

where R_\odot is the radius of the Sun.

In this work we shall neglect the effect of evaporation of the captured WIMPs from the Sun⁶, and make the standard assumption that the capture and annihilation processes have reached an approximate equilibrium state over the long lifetime of the solar system ($t_\odot \sim 4.2$ billion yrs). Under these assumptions, the total annihilation rate of WIMPs in the Sun is simply related to the total capture rate by the relation

$$\Gamma_\odot \approx \frac{1}{2} C_\odot \quad (21)$$

IV. NEUTRINO FLUX FROM WIMP ANNIHILATION IN THE SUN AND EVENT RATE IN THE DETECTOR

A. The neutrino energy spectrum

In this subsection we collect together the known results for the energy spectra of neutrinos emerging from the Sun, for various WIMP annihilation channels [43, 44, 46, 47], for use in the calculations described in the next subsection.

The differential flux of muon neutrinos observed at Earth is [43]

$$\left(\frac{d\phi_i}{dE_i} \right) = \frac{\Gamma_\odot}{4\pi D^2} \sum_F B_F \left(\frac{dN_i}{dE_i} \right)_F, \quad (i = \nu_\mu, \bar{\nu}_\mu) \quad (22)$$

where Γ_\odot is the rate of WIMP annihilation in the Sun, D is the Earth-Sun distance, F stands for the possible annihilation channels, B_F is the branching ratio for the annihilation channel F and $\left(\frac{dN_i}{dE_i} \right)_F$ is the differential energy spectrum of the neutrinos of type i emerging from the Sun resulting from the particles of annihilation

⁶ Note, however, that evaporation may not be negligible for WIMP masses below $\sim 4 \text{ GeV}$ depending on the magnitude of the annihilation cross section [36].

channel F injected at the core of the Sun. WIMPs can annihilate to all possible standard model particles e.g. e^+e^- , $\mu^+\mu^-$, $\tau^+\tau^-$, $\nu_e\bar{\nu}_e$, $\nu_\mu\bar{\nu}_\mu$, $\nu_\tau\bar{\nu}_\tau$, $\bar{q}q$ pairs and also gauge and higgs boson pairs (W^+W^- , $Z\bar{Z}$, $h\bar{h}$), etc. In this paper we are only interested in low mass ($\sim 2 - 20$ GeV) WIMPs. Therefore, we will not consider WIMP annihilations to higgs and gauge boson pairs and top quark pairs. Light quarks like u , d , s contribute very little to the energetic neutrino flux [44], and are not considered. The same is true for muons. So, in this paper we consider only the channels $\tau^+\tau^-$, $\bar{b}b$, $\bar{c}c$ and $\bar{\nu}\nu$.

The neutrino energy spectra, $\left(\frac{dN_i}{dE_i}\right)_F$, have been calculated numerically (see, e.g., [44, 45]) by considering all the details of hadronization of quarks, energy loss of the resulting heavy hadrons, neutrino oscillation effects, neutrino energy loss due to neutral current interactions and absorption due to charged current interactions with the solar medium, ν_τ regeneration, etc. However, the numerical results in [44, 45] are given for WIMP masses $m_\chi \geq 10$ GeV, and it is not obvious if those are valid for lower WIMP masses which are of our primary interest in this paper. In any case, given the presence of other uncertainties in the problem, particularly those associated with astrophysical quantities such as the local density of dark matter and its velocity distribution, we argue that it is good enough to use — as we do in this paper — approximate analytical expressions for the neutrino spectra available in the literature [43, 46, 47]. We are interested in the fluxes of muon neutrinos and antineutrinos, for which we use the analytic expressions given in Ref. [43], which neglect neutrino oscillation effects. By comparing with the neutrino fluxes obtained from detailed numerical calculations [44], we find that for small WIMP masses below ~ 20 GeV (the masses of our interest in this paper), the analytic expressions for the muon neutrino fluxes given in [43] match with the results of detailed numerical calculations [44] to within a few percent.

The main effect of the interaction of the neutrinos with the solar medium is that [47] a neutrino of type i ($= \nu_\mu, \bar{\nu}_\mu$) injected at the solar core with energy E_i^{core} emerges from the Sun with an energy E_i given by

$$E_i^{\text{core}} = E_i / (1 - E_i \tau_i), \quad (23)$$

and with probability

$$P_i = (1 + E_i^{\text{core}} \tau_i)^{-\alpha_i} = (1 - E_i \tau_i)^\alpha, \quad (24)$$

with

$$\alpha_{\nu_\mu} = 5.1, \quad \alpha_{\bar{\nu}_\mu} = 9.0, \quad \tau_{\nu_\mu} = 1.01 \times 10^{-3} \text{ GeV}^{-1}, \quad \text{and} \quad \tau_{\bar{\nu}_\mu} = 3.8 \times 10^{-4} \text{ GeV}^{-1}. \quad (25)$$

Below we write down the expressions for the energy spectra of neutrinos emerging from the Sun for the four annihilation channels considered in this paper:

1. $\tau^+\tau^-$ channel : Neutrinos from decay of τ leptons ($\tau \rightarrow \mu\nu_\mu\nu_\tau$)

For this channel, the spectrum of muon-type neutrinos at the solar surface, including the propagation effects in the solar medium, can be written as [43]

$$\left(\frac{dN_i}{dE_i}\right)_{\tau^+\tau^-} = (1 - E_i \tau_i)^{(\alpha_i - 2)} \left(\frac{dN_i^{\text{core}}}{dE_i^{\text{core}}}\right)_{\tau^+\tau^-}, \quad (i = \nu_\mu, \bar{\nu}_\mu) \quad (26)$$

where the relationship between E_i and E_i^{core} , and the values of α_i and τ_i , are as given by equations (23) and (25), respectively, and

$$\left(\frac{dN_i^{\text{core}}}{dE_i^{\text{core}}}\right)_{\tau^+\tau^-} = \frac{48 \Gamma_{\tau \rightarrow \mu\nu_\mu\nu_\tau}}{\beta \gamma m_\tau^4} \left(\frac{1}{2} m_\tau (E_i^{\text{core}})^2 - \frac{2}{3} (E_i^{\text{core}})^3 \right)_{E_-}^{\min(\frac{1}{2} m_\tau, E_+)} \quad (27)$$

is the neutrino spectrum due to decay of the τ -leptons injected at the solar core by WIMP annihilations. Here $\Gamma_{\tau \rightarrow \mu\nu_\mu\nu_\tau} = 0.18$, and $E_\pm = \frac{E_i^{\text{core}}}{\gamma(1 \mp \beta)}$ with $\gamma = (1 - \beta^2)^{-1/2} = m_\chi/m_\tau$, m_τ being the τ -lepton mass.

Note that the ν_τ s produced from τ decay may again produce τ s by charged current interactions in the solar medium, and these secondary τ s can decay to give secondary ν_μ s. But these ν_μ s would be of much lower energy compared to the primary ν_μ s from τ decay, and are not considered here.

2. $\bar{b}b$ channel : Neutrinos from decay of b -quark hadrons ($b \rightarrow c\mu\nu_\mu$)

The treatment is similar to the case of τ decay described above. However, here the hadronization of quarks and stopping of heavy hadrons in the solar medium have to be taken into account. The resulting spectrum of muon-neutrinos emerging from the Sun is given by [43]

$$\left(\frac{dN_i}{dE_i}\right)_{\bar{b}b} = \int_{m_b}^{E_0} \left(\frac{1}{N} \frac{dN}{dE_d}\right)^{\text{hadron}}(E_0, E_d) (1 - E_i \tau_i)^{(\alpha_i-2)} \left(\frac{dN_i^{\text{core}}}{dE_i^{\text{core}}}\right)_{\bar{b}b}(E_d, E_i^{\text{core}}) dE_d, \quad (i = \nu_\mu, \bar{\nu}_\mu) \quad (28)$$

where m_b is the b -quark mass, $E_0 \approx 0.71m_\chi$ is the initial energy of the b -quark hadron (the fragmentation function is assumed to be a sharply peaked function [43]),

$$\left(\frac{dN_i^{\text{core}}}{dE_i^{\text{core}}}\right)_{\bar{b}b}(E_d, E_i^{\text{core}}) = \frac{48 \Gamma_{b \rightarrow \mu\nu_\mu X}}{\beta \gamma m_b^4} \left(\frac{1}{2} m_b (E_i^{\text{core}})^2 - \frac{2}{3} (E_i^{\text{core}})^3\right)_{E_-}^{\min(\frac{1}{2} m_b, E_+)} \quad (29)$$

is the neutrino spectrum resulting from decay of the b -quark hadron injected at the solar core, and

$$\left(\frac{1}{N} \frac{dN}{dE_d}\right)^{\text{hadron}}(E_0, E_d) = \frac{E_c}{E_d^2} \exp\left[\frac{E_c}{E_0} - \frac{E_c}{E_d}\right], \quad (30)$$

with $E_c \approx 470 \text{ GeV}$, is the distribution of the hadron's energy at the time of its decay if it is produced with an initial energy E_0 . In equation (29), $\Gamma_{b \rightarrow \mu\nu_\mu X} = 0.103$ is the branching ratio for inclusive semi-leptonic decay of b -quark hadrons to muons [48], and $E_\pm = \frac{E_i^{\text{core}}}{\gamma(1 \mp \beta)}$ with $\gamma = (1 - \beta^2)^{-1/2} = E_d/m_b$.

3. $\bar{c}c$ channel : Neutrinos from decay of c -quark hadrons ($c \rightarrow s\mu\nu_\mu$)

Again, this is similar to the case of b -decay discussed above, except that the kinematics of the process is slightly different. The resulting muon neutrino spectrum is given by [43]

$$\left(\frac{dN_i}{dE_i}\right)_{\bar{c}c} = \int_{m_c}^{E_0} \left(\frac{1}{N} \frac{dN}{dE_d}\right)^{\text{hadron}}(E_0, E_d) (1 - E_i \tau_i)^{(\alpha_i-2)} \left(\frac{dN_i^{\text{core}}}{dE_i^{\text{core}}}\right)_{\bar{c}c}(E_d, E_i^{\text{core}}) dE_d, \quad (i = \nu_\mu, \bar{\nu}_\mu) \quad (31)$$

where m_c is the c -quark mass, $E_0 \approx 0.55m_\chi$ is the initial energy of the charmed hadron,

$$\left(\frac{dN_i^{\text{core}}}{dE_i^{\text{core}}}\right)_{\bar{c}c}(E_d, E_i^{\text{core}}) = \frac{8 \Gamma_{c \rightarrow \mu\nu_\mu X}}{\beta \gamma m_c^4} \left(\frac{3}{2} m_c (E_i^{\text{core}})^2 - \frac{4}{3} (E_i^{\text{core}})^3\right)_{E_-}^{\min(\frac{1}{2} m_c, E_+)} \quad (32)$$

is the neutrino spectrum resulting from decay of the c -quarks injected at the solar core, with $\Gamma_{c \rightarrow \mu\nu_\mu X} = 0.13$, $E_\pm = \frac{E_i^{\text{core}}}{\gamma(1 \mp \beta)}$, $\gamma = (1 - \beta^2)^{-1/2} = E_d/m_c$, and $\left(\frac{1}{N} \frac{dN}{dE_d}\right)^{\text{hadron}}(E_0, E_d)$ is given by equation (30) with $E_c \approx 250 \text{ GeV}$ for c -quark.

4. $\nu\bar{\nu}$ channel : ($\chi\chi \rightarrow \nu_\mu \bar{\nu}_\mu$)

In this case the spectrum of muon neutrinos emerging from the Sun is simply given by

$$\left(\frac{dN_i}{dE_i}\right)_{\nu\bar{\nu}} = (1 - E_i \tau_i)^{(\alpha_i-2)} \left(\frac{dN_i^{\text{core}}}{dE_i^{\text{core}}}\right)_{\nu\bar{\nu}}, \quad (i = \nu_\mu, \bar{\nu}_\mu) \quad (33)$$

where

$$\left(\frac{dN_i^{\text{core}}}{dE_i^{\text{core}}}\right)_{\nu\bar{\nu}} = \delta(E_i^{\text{core}} - m_\chi) \equiv (1 + m_\chi \tau_i)^{-2} \delta\left(E_i - \frac{m_\chi}{1 + m_\chi \tau_i}\right). \quad (34)$$

B. Calculation of Event Rates in the Super-Kamiokande detector

The rate of neutrino induced upward-going muon events, \mathcal{R} , in the S-K detector due to ν_μ s and $\bar{\nu}_\mu$ s from WIMP annihilation in the Sun can be written as

$$\mathcal{R} = \frac{1}{2} \sum_{i=\nu_\mu, \bar{\nu}_\mu} \int \int \frac{d\phi_i}{dE_i} \frac{d\sigma_{iN}}{dy}(E_i, y) V_{\text{eff}}(E_\mu) n_p^{\text{water}} dE_i dy, \quad (35)$$

where $\frac{d\phi_i}{dE_i}$ is the differential flux of the neutrinos given by equation (22), $\frac{d\sigma_{iN}}{dy}$ are the relevant neutrino-nucleon charged current differential cross sections, $(1-y) (= E_\mu/E_i)$ is the fraction of the neutrino energy transferred to the muon, $V_{\text{eff}}(E_\mu)$ is the effective volume of the detector, and n_p^{water} is the number density of protons in water (= Avogadro number). The S-K Collaboration imposed a cut on the upward-going muon path-length of > 7 meters in the inner detector which has an effective area of $A_{\text{eff}} \approx 900 \text{ m}^2$ and height ≈ 36.2 m. This 7-meter cut on the muon track length can be effectively taken into account by setting $V_{\text{eff}} = 0$ if the effective water-equivalent muon range, $R_\mu(E_\mu) \approx 5 \text{ meters} \times (E_\mu/\text{GeV})$, is less than 7 meters, and $V_{\text{eff}} = A_{\text{eff}} \times [R_\mu(E_\mu) + (36.2 - 7) \text{ meters}]$ otherwise [36]. The factor of 1/2 accounts for the fact that only up-going muon events were considered in order to avoid the background due to down-going muons produced due to cosmic ray interactions in the Earth's atmosphere.

The S-K muon events were broadly classified into three categories [49], namely, (i) Fully Contained (FC), (ii) Stopping (S) and (iii) Through-Going (TG) events. For ν_μ energy $\lesssim 4 \text{ GeV}$ the events are predominantly of FC type, whereas for ν_μ energy $\gtrsim 8 \text{ GeV}$ the events are predominantly of TG type. Assuming that annihilation of the WIMP of mass m_χ produces neutrinos of typical energy $\sim (\frac{1}{3} - \frac{1}{2})m_\chi$, we can roughly divide the m_χ range of our interest into three regions according to the resulting muon event types namely, (i) $2 \lesssim m_\chi \lesssim 8 \text{ GeV}$ (FC), (ii) $8 \lesssim m_\chi \lesssim 15 \text{ GeV}$ (FC + S) and (iii) $15 \text{ GeV} \lesssim m_\chi$ (FC + S + TG).

To set upper limits on the WIMP elastic scattering cross section as a function of WIMP mass for a given annihilation channel, we use the following 90% C.L. upper limits [18, 19] on the rates of the upgoing muon events of the three different types mentioned above:

$$\begin{aligned} \mathcal{R}_{\text{FC}}^{90\% \text{ C.L.}} &\simeq 13.8 \text{ yr}^{-1}, \\ \mathcal{R}_{\text{S}}^{90\% \text{ C.L.}} &\simeq 1.24 \text{ yr}^{-1}, \\ \mathcal{R}_{\text{TG}}^{90\% \text{ C.L.}} &\simeq 0.93 \text{ yr}^{-1}. \end{aligned} \quad (36)$$

The upper limits on the WIMP-nucleon elastic scattering cross section so derived are then translated into upper limits on the branching fractions of various annihilation channels by demanding the consistency of DAMA-compatible region of the WIMP parameter space with S-K upper limits. These limits are discussed in the next section.

V. RESULTS AND DISCUSSIONS

Fig. 1 shows the dependence of the capture rate of WIMPs by the Sun as a function of the WIMP's mass for the three halo models specified in Table I. As expected, for a given DM density, the capture rate decreases as WIMP mass increases because heavier WIMPs correspond to smaller number density of WIMPs.

The event rates in the S-K detector as a function of the WIMP mass for the four different WIMP annihilation channels are shown in Figure 2 assuming 100% branching ratio for each channel by itself. For each annihilation channel the three curves correspond, as indicated, to the three halo models specified in Table I. It is seen that the direct annihilation to the $\nu\bar{\nu}$ channel dominates the event rate, followed by the $\tau^+\tau^-$ channel.

Our main results are contained in Figures 3, 4 and 5, where we show, for the three halo models considered, the 90% C.L. upper limits on the WIMP-proton SI and SD elastic cross sections (as a function of WIMP mass) derived from the Super-Kamiokande measurements of the up-going muon events from the direction of the Sun [18, 19], for the four annihilation channels discussed in the text, assuming 100% branching ratio for each channel by itself. In these Figures, we also display, for the respective halo models, the 90% C.L. allowed regions [15] in the WIMP mass vs. WIMP-proton elastic cross section plane implied by the DAMA/LIBRA collaboration's claimed annual modulation signal [6], as well

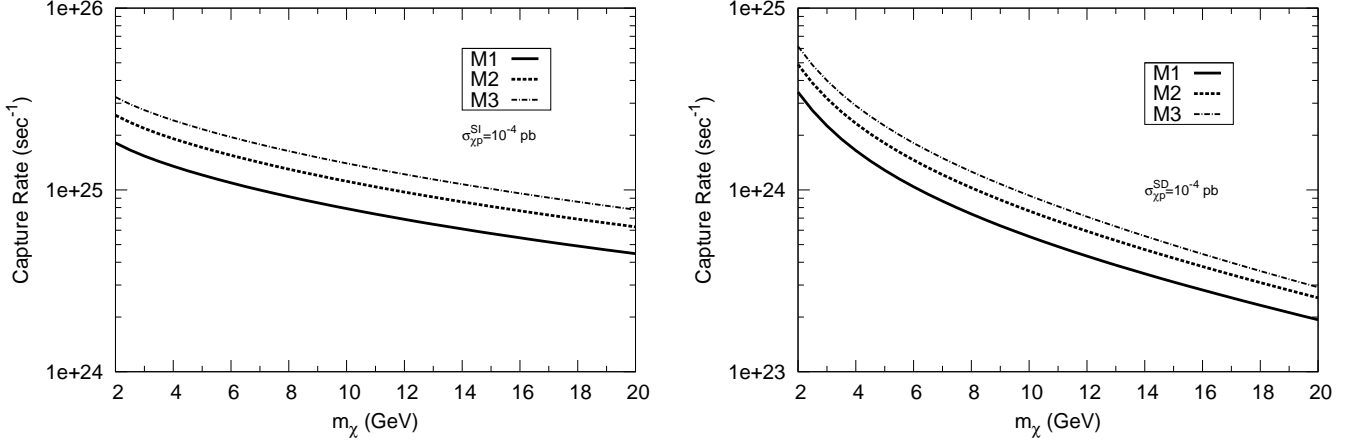


FIG. 1: The capture rate as a function of the WIMP mass for the three halo models specified in Table I, and for spin-independent (SI: left panel) and spin-dependent (SD: right panel) WIMP-proton interactions. All the curves are for a reference value of the WIMP-proton elastic SI or SD cross section of 10^{-4} pb.

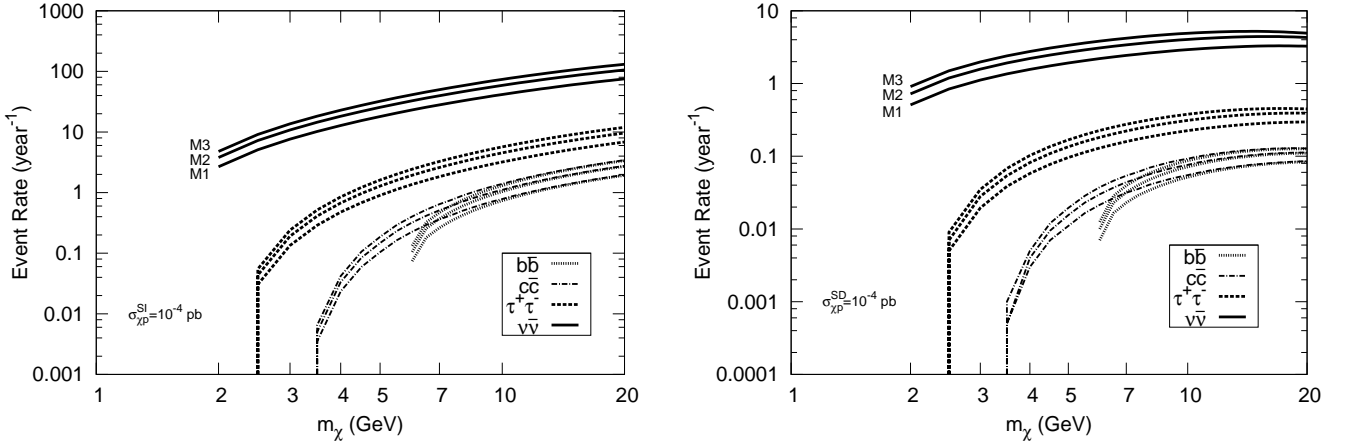


FIG. 2: The upward going muon event rates in the Super-Kamiokande detector due to neutrinos from WIMP annihilation in the Sun as a function of the WIMP mass for the four annihilation channels as indicated, assuming 100% branching ratios for each channel by itself, and for spin-independent (SI: left panel) and spin-dependent (SD: right panel) WIMP-proton interactions. The three curves for each annihilation channel correspond, as indicated, to the three halo models specified in Table I. All the curves are for a reference value of the WIMP-proton elastic SI or SD cross section of 10^{-4} pb.

as the 90% C.L. upper limits [15] on the relevant cross section as a function of the WIMP mass implied by the null results from the CRESST-1 [50], CDMS-II-Si [12], CDMS-II-Ge [51] and XENON10 [10] experiments.

The curves in Figures 3, 4 and 5 allow us to derive upper limits on the branching fractions of the various WIMP annihilation channels, from the requirement of consistency of the S-K-implied upper limits on the WIMP-proton elastic cross section with the DAMA-compatible regions. These upper limits are shown in Table II for the three halo models discussed in the text.

Clearly, for the case of spin-independent interaction, there are no constraints on the branching fractions for the $b\bar{b}$ and $c\bar{c}$ channels since the DAMA-compatible region is already consistent with the S-K upper limit even for 100% branching fractions in these channels (the respective curves for the various annihilation channels only move upwards, keeping the shape same, as the branching fractions are made smaller). At the same time, for the $\tau^+\tau^-$ channel and SI interaction, although a 100% branching fraction in this channel allows a part of the DAMA-compatible region to

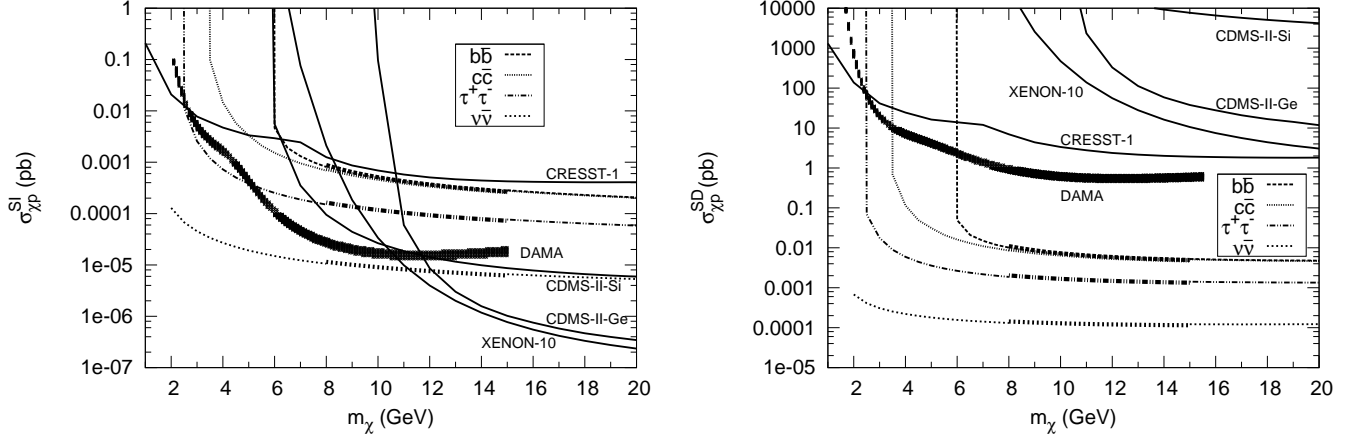


FIG. 3: The 90% C.L. upper limits on the WIMP-proton spin-independent (SI: left panel) and spin-dependent (SD: right panel) elastic cross section as a function of WIMP mass derived from the Super-Kamiokande measurements of the up-going muon events from the direction of the Sun [18, 19], for the three relevant event types, namely, Fully Contained (FC), Stopping (S) and Through Going (TG), as discussed in the text (see Eq.[36]). The thick portions of the curves serve to demarcate the approximate m_χ ranges where the different event types make dominant contributions to the upper limits. The curves shown are for the four annihilation channels, assuming 100% branching ratio for each channel by itself. The 90% C.L. allowed regions in the WIMP mass vs. WIMP-proton elastic cross section plane implied by the DAMA/LIBRA experiment's claimed annual modulation signal [6] as well as the 90% C.L. upper limits on the cross section as a function of the WIMP mass implied by the null results from the CRESST-1 [50], CDMS-II-Si [12], CDMS-II-Ge [51] and XENON10 [10] experiments (solid curves) are also shown. All the curves shown are for our halo model M1 ($\rho_{\text{DM},\odot} = 0.2 \text{ GeV/cm}^3$) specified in Table I.

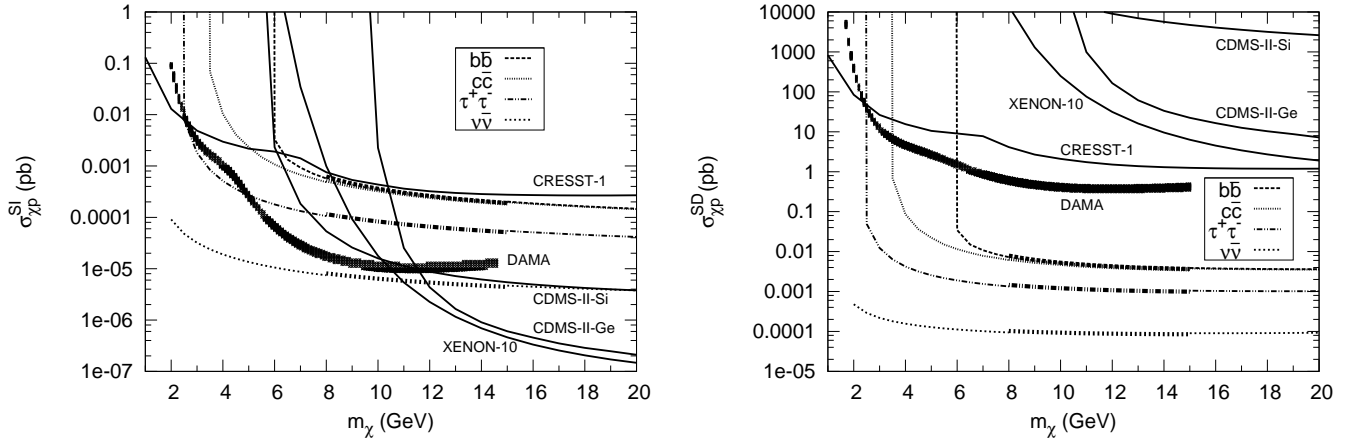


FIG. 4: Same as Fig. 3, but for the halo model M2 ($\rho_{\text{DM},\odot} = 0.3 \text{ GeV/cm}^3$) specified in Table I.

be consistent with the S-K upper limit, consistency of the *entire* DAMA-compatible region with the S-K upper limit requires the branching fraction for this channel to be less than 35–45% depending on the halo model. On the other hand, for the $\nu\bar{\nu}$ channel and SI interaction, there are already strong upper limits (at the level of 25 – 35%) on the branching fraction for this channel for consistency of even a part of the DAMA-compatible region with the S-K upper limit; and these upper limits become significantly more stringent (by about two orders of magnitude) if the entire DAMA-compatible region is required to be consistent with the S-K upper limits.

The constraints on the branching fractions of various annihilation channels are, however, much more severe in the case of spin-dependent interaction: For the quark channels, only parts of the DAMA-compatible region can be made consistent with the S-K upper limits, and that only if the branching fractions for these channels are restricted at the

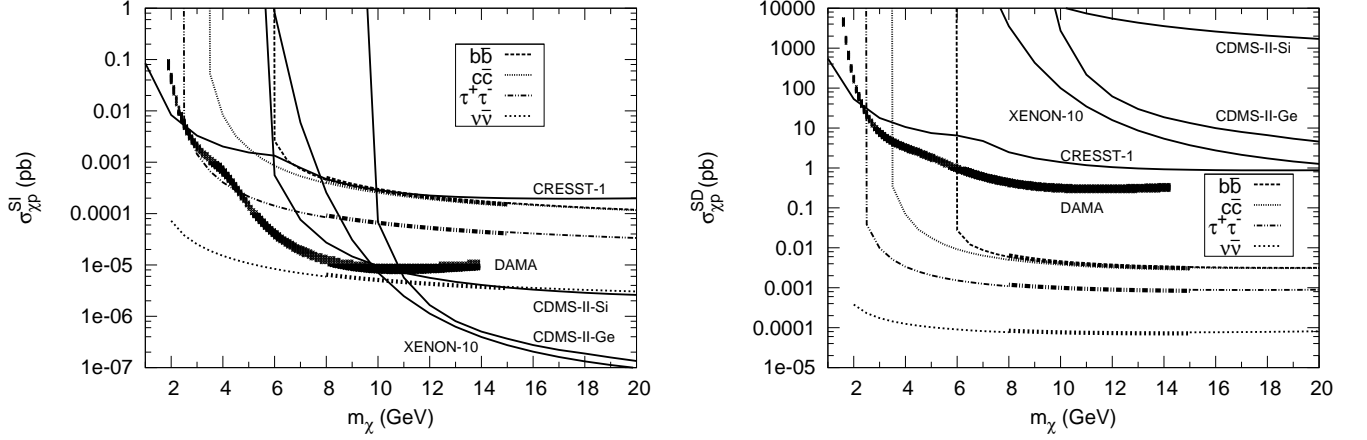


FIG. 5: Same as Fig. 3, but for the halo model M3 ($\rho_{\text{DM},\odot} = 0.4 \text{ GeV/cm}^3$) specified in Table I.

	EVENT TYPE (m_χ range in GeV)	UPPER LIMITS ON THE BRANCHING FRACTIONS (in %) (M1, M2, M3)			
		$b\bar{b}$	$c\bar{c}$	$\tau^+\tau^-$	$\nu\bar{\nu}$
SI	FC (2.0 – 8.0)	100, 100, 100	100, 100, 100	35, 40, 45	0.4, 0.6, 0.8
	FC+S (8.0 – 15.0)	100, 100, 100	100, 100, 100	100, 100, 100	25, 30, 35
	FC+S+TG (15.0 – 20.0)	100, 100, 100	100, 100, 100	100, 100, 100	25, 30, 35
SD	FC (2.0 – 8.0)	0.5, 0.6, 0.7	0.5, 0.6, 0.7	0.05, 0.06, 0.07	0.0005, 0.0006, 0.0007
	FC+S (8.0 – 15.0)	0.6, 0.7, 0.8	0.6, 0.7, 0.8	0.14, 0.16, 0.18	0.012, 0.014, 0.016
	FC+S+TG (15.0 – 20.0)	0.6, 0.7, 0.8	0.6, 0.7, 0.8	0.14, 0.16, 0.18	0.012, 0.014, 0.016

TABLE II: Upper limits — derived from Figures 3, 4 and 5 — on the branching fractions for the four annihilation channels, from the requirement of consistency of the S-K implied upper limits on the WIMP-proton elastic cross sections with the “DAMA-compatible” region of the WIMP mass versus cross section parameter space (within which the annual modulation signal observed by the DAMA/LIBRA experiment [6] is compatible with the null results of other DD experiments determined within the context of our halo model [15]), for both spin-independent (SI) and spin-dependent (SD) interactions and the three halo models specified in Table I. The limits are calculated using the three different upward-going muon event types, namely, Fully Contained (FC), Stopping (S) and Through Going (TG). The three consecutive numbers for each annihilation channel and muon event type refer to the three different halo models M1, M2, M3, as indicated.

level of (0.6 – 0.8)%. On the other hand, for $\tau^+\tau^-$ and $\nu\bar{\nu}$ channels, parts of the DAMA-compatible regions can be consistent with S-K upper limits only if their branching fractions are restricted at the level of (0.14 – 0.18)% and (0.012 – 0.016)%, respectively, while consistency of the entire DAMA-compatible regions with the S-K upper limits requires these fractions to be respectively lower by about a factor of 2.5 (for the $\tau^+\tau^-$ channel) and a factor of about 25 (for the $\nu\bar{\nu}$ channel).

The above small numbers for the upper limits on the branching fractions of the four dominant neutrino producing WIMP annihilation channels imply, in the case of spin-dependent WIMP interaction, that the DAMA-allowed region of the $m_\chi - \sigma_{\chi p}^{\text{SD}}$ parameter space is essentially ruled out by the S-K upper limit on neutrinos from possible WIMP annihilations in the Sun, unless, of course, WIMPs efficiently evaporate from the Sun — which may be the case for relatively small mass WIMPs below 4 GeV [36] — or there are other non-standard but dominant WIMP annihilation channels that somehow do not eventually produce any significant number of neutrinos while restricting annihilation to quark ($b\bar{b}$, $c\bar{c}$) channels to below 0.5% level and $\tau^+\tau^-$ and $\nu\bar{\nu}$ channels to below 0.05% and 0.0005% level, respectively. In the case of spin-independent interaction, however, the DAMA-compatible region of the $m_\chi - \sigma_{\chi p}^{\text{SI}}$ parameter space (or at least a part thereof) remains unaffected by the S-K upper limit if WIMPs annihilate dominantly to quarks and/or tau leptons, and annihilation directly to neutrinos is restricted below $\sim (25 - 35)\%$ level. At the same time, portions of the DAMA-compatible region can be excluded if WIMP annihilation to $\tau^+\tau^-$ occurs at larger than (35 – 45)% level and/or annihilation to $\nu\bar{\nu}$ occurs at larger than (0.4 – 0.8)% level. These results, based as they are on a self-consistent model of the Galaxy’s dark matter halo, the parameters of which are determined by a fit to the

rotation curve of the Galaxy, strengthen, at the qualitative level, the earlier conclusion within the SHM that the S-K upper limit on the possible flux of neutrinos due to WIMP annihilation in the Sun severely restricts the DAMA region of the WIMP mass versus cross section plane, especially in the case of spin-dependent interaction of WIMPs with nuclei, although the quantitative restrictions on the WIMP cross section and branching fractions of various WIMP annihilation channels obtained here are different (in some cases by more than a factor of 10) from those obtained in earlier calculations within the SHM.

Note added: After the completion of the main calculations of the present work, new results of the S-K collaboration’s search for upward-going muons (“upmus”) due to neutrinos from Sun [20] have appeared. These new results are based on a data set consisting of 3109.6 days of data, nearly double the size of the old data set of 1679.6 days used in Ref. [18] and in the analysis of this paper so far. Here we consider these new results of Ref. [20] and the resulting changes to the constraints on various WIMP annihilation channels derived above using the earlier S-K results. In general, we find that with the new S-K results the upper limits on the branching fractions of various annihilation channels become more stringent by a factor of 3 – 4 than those derived above.

The upmu event categories used in the new S-K paper [20] are somewhat different from those in their earlier work [18]. These are: “stopping” (S), “non-showering through-going” (NSTG), and “showering through-going” (STG); see Ref. [20] for details. For a given WIMP mass, Figure 2 of Ref. [20] allows us to read out the fraction of each upmu event type contributing to the total number of events, from the consideration that the typical maximum energy of a neutrino produced in the annihilation of a WIMP of mass m_χ is $\sim m_\chi/2$. For low WIMP masses of our interest in this paper, $m_\chi \lesssim 20$ GeV (and hence typical neutrino energies $\lesssim 10$ GeV), the stopping events dominate and constitute more than 70% of the total number of upmu events, as clear from Figure 2 of Ref. [20]. It is thus expected, as indeed we do find from our calculations, that the most stringent upper limits on the branching fractions of various WIMP annihilation channels for low WIMP masses come from the observed rate of these Stopping events.⁷

The 90% C.L. Poissonian upper limit on the rate of these Stopping-type upmu events for the new data set of Ref. [20], estimated from the total number of this type of upmu events and the number of background upmus due to atmospheric neutrinos given in Figure 3 of that reference, is ⁸ $\sim 3.27 \text{ yr}^{-1}$. With this, we can calculate, as we did in the analysis above, the 90% C.L. upper limits on the WIMP-proton SI and SD elastic cross sections as a function of WIMP mass for the new S-K data set of Ref. [20], for the case of 100% branching ratio for each of the four annihilation channels considered above. The results, for our best-fit halo model M1, are shown in Figure 6.

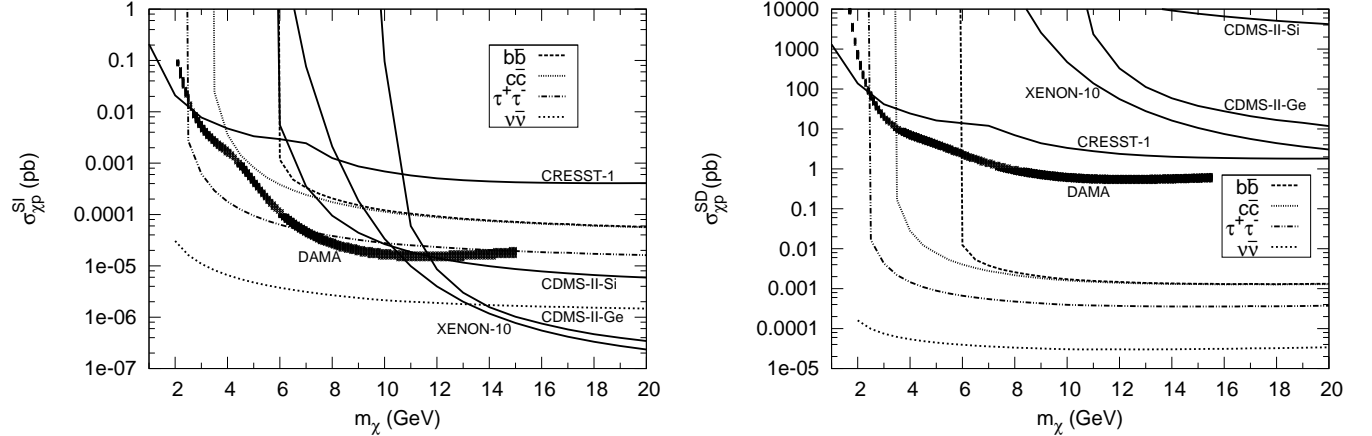


FIG. 6: Same as Fig. 3, but using the new S-K data from Ref. [20] and considering their “Stopping” upmu events only.

⁷ Recall that, for the older data set [18], the most stringent upper limits came from the fully-contained (FC) events; see Table II above.
⁸ We take the events in the 0–30 degree cone half-angle bin around the Sun to be consistent with the analysis done above for the earlier S-K data set.

The resulting upper limits on the branching fractions of the four annihilation channels, derived from the requirement of consistency of the new S-K-implied upper limits on the WIMP-proton elastic cross sections shown in Figure 6 with the “DAMA-compatible” regions, are displayed in Table III. A comparison with the corresponding numbers given in

	Upper limits on the branching fractions (in %) from “Stopping” events, with halo model M1			
	$\bar{b}b$	$\bar{c}c$	$\tau^+\tau^-$	$\nu\bar{\nu}$
SI	100	100	10	0.11
SD	0.12	0.12	0.012	0.00013

TABLE III: Upper limits on the branching fractions of the four annihilation channels, derived from the requirement of consistency of the new S-K-implied upper limits on the WIMP-proton elastic cross sections shown in Figure 6 with the “DAMA-compatible” regions, for both spin-independent (SI) and spin-dependent (SD) interactions

Table II shows that the new upper limits on the branching fractions for the relevant annihilation channels are roughly a factor of 3–4 more stringent.

VI. SUMMARY

Several studies in recent years have brought into focus the possibility that the dark matter may be in the form of a relatively light WIMP of mass in the few GeV range. Such light WIMPs with suitably chosen values of the WIMP-nucleon SI or SD elastic cross section can be consistent with the annual modulation signal seen in the DAMA/LIBRA experiment [6] without conflicting with the null results of other direct-detection experiments. To further probe the “DAMA-compatible” regions of the WIMP parameter space — the regions of the WIMP mass versus cross section parameter space within which the annual modulation signal observed by the DAMA/LIBRA experiment is compatible with the null results of other DD experiments — we have studied in this paper the independent constraints on the WIMP-proton SI as well as SD elastic scattering cross section imposed by the upper limit on the neutrino flux from WIMP annihilation in the Sun given by the Super-Kamiokande experiment [18, 19]. Assuming approximate equilibrium between the capture and annihilation rates of WIMPs in the Sun, we have calculated the 90% C.L. upper limits on the WIMP-proton SI and SD elastic cross sections as a function of the WIMP mass for various WIMP annihilation channels using the Super-Kamiokande upper limits, and examined the consistency of those limits with the 90% C.L. “DAMA-compatible” regions. This we have done within the context of a self-consistent phase-space model of the finite-size dark matter halo of the Galaxy, namely, the Truncated Isothermal Model (TIM) [15, 23], in which we take into account the mutual gravitational interaction between the dark matter and the observed visible matter in a self-consistent manner, with the parameters of the model determined by a fit to the observed rotation curve data of the Galaxy.

We find that the requirement of consistency of the S-K [18, 19] implied upper limits on the WIMP-proton elastic cross section as a function of WIMP mass imposes stringent restrictions on the branching fractions of the various WIMP annihilation channels. In the case of spin-independent WIMP-proton interaction, the S-K upper limits do not place additional restrictions on the DAMA-compatible region of the WIMP parameter space if the WIMPs annihilate dominantly to $\bar{b}b$ and $\bar{c}c$, and if direct annihilations to $\tau^+\tau^-$ and neutrinos are restricted to below $\sim (35 - 45)\%$ and $(0.4 - 0.8)\%$, respectively. In the case of spin-dependent interactions, on the other hand, the restrictions on the branching fractions of various annihilation channels are much more stringent, essentially ruling out the DAMA-compatible region of the WIMP parameter space if the relatively low-mass WIMPs under consideration annihilate predominantly to any mixture of $\bar{b}b$, $\bar{c}c$, $\tau^+\tau^-$, and $\nu\bar{\nu}$ final states. The very latest results from the S-K Collaboration [20] put the above conclusions on an even firmer footing by making the above constraints on the branching fractions of various WIMP annihilation channels more stringent by roughly a factor of 3–4. Similar conclusions were reached earlier [19, 36] within the context of the SHM. The quantitative restrictions on the branching fractions for various WIMP annihilation channels obtained here and as given in Table II (and in Table III for the latest S-K results [20]) are, however, significantly different from those in the earlier works.

An important aspect of the Truncated Isothermal model of the Galactic halo used in the present calculation is the *non-Maxwellian nature of the WIMP velocity distribution* in this model, as opposed to the Maxwellian distribution in the SHM (see Ref. [15] for details). This directly affects the WIMP capture rate (and consequently the annihilation rate), resulting in significant quantitative differences in the values of the upper limits on the WIMP-proton elastic

cross sections (implied by the S-K upper limits on the neutrinos from the Sun) compared to the values in the SHM. Similarly, the upper limits on the branching fractions of various possible WIMP annihilation channels (from the requirement of compatibility with DAMA results) are also changed. At a qualitative level, however, the general conclusion reached earlier [19, 36] within the context of the SHM — that S-K upper limits on neutrinos from the Sun severely restrict the DAMA-compatible region of the WIMP parameter space — remains true in the present model too, thus adding robustness to this conclusion.

Acknowledgments

We thank Soumini Chaudhury, Martin Winkler and Dan Hooper for useful discussions and communications.

Bibliography

- [1] G. Jungman, M. Kamionkowski and K. Griest, Phys. Rep. **267** (1996) 195 [arXiv:hep-ph/9506380].
- [2] L. Bergstrom, Rep. Prog. Phys. **63** (2000) 793 [arXiv:hep-ph/0002126].
- [3] G. Bertone, D. Hooper and J. Silk, Phys. Rep. **405** (2005) 279.
- [4] D. Hooper and S. Profumo, Phys. Rep. **453** (2007) 29.
- [5] G. Bertone (Ed.), Particle Dark Matter: Observations, Models and Searches (Cambridge Univ. Press, U. K., 2010).
- [6] DAMA/LIBRA collaboration: R. Bernabei et al., Eur. Phys. J. **C 56** (2008) 333 [arXiv:0804.2741]; *ibid* **C 67** (2010) 39 [arXiv:1002.1028].
- [7] CoGeNT collaboration: C.E. Aalseth et al, Phys. Rev. Lett. **106** (2011) 131301 [arXiv:1002.4703].
- [8] D. Hooper, J.I. Collar, J. Hall, D. McKinsey and C.M. Kelso, Phys. Rev. **D 82** (2010) 123509 [arXiv:1007.1005].
- [9] A.L. Fitzpatrick, D. Hooper, K.M. Zurek, Phys. Rev. **D 81** (2010) 115005 [arXiv:1003.0014].
- [10] XENON10 collaboration: J. Angle et al., Phys. Rev. **D 80** (2009) 115005 [arXiv:0910.3698].
- [11] XENON100 collaboration: E. Aprile et al., Phys. Rev. Lett. **105** (2010) 131302 [arXiv:1005.0380].
- [12] CDMS collaboration, D.S. Akerib et al., Phys. Rev. Lett. **96** (2006) 011302 [arXiv:astro-ph/0509259].
- [13] F.J. Petriello and K. M. Zurek, JHEP **09** (2008) 047 [arXiv:0806.3989].
- [14] C. Savage, G. Gelmini, P. Gondolo and K. Freese, JCAP **04** (2009) 010 [arXiv:0808.3607].
- [15] S. Chaudhury, P. Bhattacharjee, R. Cowsik, JCAP **09** (2010) 020 [arXiv:1006.5588].
- [16] CDMS collaboration: Z. Ahmed et al., Phys. Rev. Lett. **106** (2011) 131302 [arXiv:1011.2482].
- [17] XENON100 collaboration: E. Aprile et al., arXiv:1104.2549.
- [18] Super-Kamiokande collaboration: S. Desai et al, Phys. Rev. **D 70** (2004) 083523 .
- [19] R. Kappl and M.W. Winkler, Nucl. Phys. B. **850** (2011) 505 [arXiv:1104.0679].
- [20] Super-Kamiokande collaboration: T. Tanaka et al, Astrophys. J. **742**:78 (2011) [arXiv:1108.3384].
- [21] D. Hooper, L. Goodenough, Phys. Lett. **B 697** (2011) 412 [arXiv:1010.2752].
- [22] A. Boyarsky, D. Malyshev, O. Ruchayskiy, [arXiv:1012.5839].
- [23] R. Cowsik, C. Ratnam, P. Bhattacharjee and S. Majumdar, New Astron. **12** (2007) 507.
- [24] M. Honma and Y. Sofue, PASJ **49** (1997) 453.
- [25] X.X. Xue et al., Astrophys. J. **684** (2008) 1143 (2008).
- [26] J. Binney and S. Tremaine, Galactic Dynamics, 2nd Edition (Princeton University Press, Princeton, 2008).
- [27] K. Freese, J.A. Frieman and A. Gould, Phys. Rev. **D 37** (1988) 3388.
- [28] J.D. Lewin and R.F. Smith, Astropart. Phys. **6** (1996) 87.
- [29] J.H. Oort, Bull. Astr. Inst. Netherlands **6** (1937) 249; *ibid.* **15** (1960) 45.
- [30] N. Bahcall, Astrophys. J. **276** (1984) 169.
- [31] P. Salucci, F. Nesti, G. Gentile and C.F. Martins, A&A **523** (2010) A83 [arXiv:1003.3101].
- [32] F.-S. Ling, E. Nezri, E. Athanassoula and R. Teyssier, JCAP **02** (2010) 012 [arXiv:0909.2028].
- [33] R. Catena and P. Ullio, JCAP **08** (2010) 004 [arXiv:0907.0018].
- [34] P.J. McMillan, MNRAS **414**, 2446 (2011) [arXiv:1102.4340].
- [35] M.J. Reid et al., Astrophys. J. **700** (2009) 137 [arXiv:0902.3913].
- [36] D. Hooper, F. Petriello, K.M. Zurek, and M. Kamionkowski, Phys. Rev. **D 79** (2009) 015010 [arXiv:0808.2464].
- [37] J. Feng, J. Kumar, J. Learned and L. Strigari, JCAP **01** (2009) 032 [arXiv:0808.4151].
- [38] V. Niro, A. Bottino, N. Fornengo and S. Scopel, Phys. Rev. **D80** (2009) 095019 [arXiv:0909.2348].
- [39] S.M. Koushiappas and M. Kamionkowski, Phys. Rev. Lett. **103** (2009) 121301 [arXiv:0907.4778].
- [40] A. Gould. Astrophys. J. **321** (1987) 571.
- [41] W. Press and D. Spergel, Astrophys. J. **296** (1985) 679.
- [42] S. Chaudhuri and P. Bhattacharjee, in preparation.
- [43] G. Jungman and M. kamionkowski, Phys. Rev. D **51** (1995) 328.
- [44] M. Cirelli et al, Nucl. Phys. B **727** (2005) 99; Erratum: *ibid* **790** (2008) 338.
- [45] J. Edsjö, WimpSim Neutrino Monte Carlo, <http://www.physto.se/~edsjo/wimpsim/>.
- [46] T.K. Gaisser, G. Steigman and S. Tilav, Phys. Rev. **D 34** (1986) 2206.

- [47] S. Ritz and D. Seckel, Nucl. Phys. B **304** (1988) 877.
- [48] Particle Data Group, K. Hikasa et al., Phys. Rev. **D 45** (1992) S1, Erratum: *ibid* **D 46** (1992) 5210.
- [49] Super-Kamiokande collaboration: Y. Ashie et al, Phys. Rev. **D 71** (2005) 112005.
- [50] G. Angloher et al., Astropart. Phys. **18** (2002) 43.
- [51] CDMS collaboration, Z. Ahmed et al., Phys. Rev. Lett. **102** (2009) 011301 [arXiv:0802.3530].